JOURNAL OF MATERIALS SCIENCE 19 (1984) 2749–2770

# SiC filament/titanium matrix composites regarded as model composites

## Part 2 *Fibre/matrix chemical interactions at high temperatures*

P. MARTINEAU, R. PAILLER, M. LAHAYE, R. NASLAIN
*Laboratoire de Chimie du Solide du CNRS, Université de Bordeaux I, 351, Cours de la Libération, 33405, Talence, France*

It is generally accepted that silicon carbide CVD-filaments are more suitable than the related boron filaments for reinforcing titanium alloys at medium temperatures. Silicon carbide has a higher refractoriness and chemical inertia than boron. Moreover, the SiC CVD-filaments retain a much higher fraction of their room temperature mechanical performances up to about 800 to 1000° C and could be produced in the future at a lower price. Despite the fact that SiC seems to be less reactive than boron towards most metals, it nevertheless reacts with titanium and its alloys at rather low temperatures (700 to 800° C). Furthermore, silicon carbide when deposited from a gas phase (e.g. methyl chlorosilane and hydrogen mixtures) often contains small amounts of more reactive species such as elemental silicon or carbon. In the same manner, coatings containing elemental carbon have been applied to SiC CVD-filaments in order to reduce their sensitivity to surface abrasion effects. Therefore, SiC filament–titanium matrix composites must be regarded as non-equilibrium systems when they are heated at medium or high temperatures. The occurrence of chemical interactions between SiC and titanium in the solid state, controlled by diffusion, has already been established either from experiments performed on diffusion couples with a plane interface [1, 2] or on fibrous composite samples [3–12]. However, the nature of the phases and the growth mechanism of the filament–matrix (FM) reaction zone remains a subject of controversy. The aim of the present contribution is to analyse, for various well characterized SiC-based CVD-filaments (stoichiometric SiC, SiC with a pyrocarbon coating, SiC with a SiC + C coating) and titanium matrices (unalloyed titanium or Ti–6Al–4V): (a) the FM interaction zone composition, (b) its kinetics of growth in the 700 to 1100° C temperature range, and (c) the growth mechanism. The filaments which have been used here have been carefully analysed previously on a chemical, microstructural and mechanical point of view in Part 1. In the same manner, the results of the present study on FM chemical interaction will be later correlated with those of different mechanical characterizations [13, 14].

## 1. Materials synthesis and analysis

Three types of SiC-based CVD-filaments have been utilized for the synthesis of the composite samples used in this study:

1. stoichiometric SiC-filaments (100 $\mu$m diameter with a 12 $\mu$m tungsten core) produced a few years ago by SNPE (Paris) on a development level and referred to as SiC(3);

2. two SiC-based filaments (140 $\mu$m diameter with a ~ 35 $\mu$m carbon core) produced by AVCO (Lowell, Mass.) in the more recent past. Both are characterized by an inner shell of SiC + C deposit and an outer shell of almost stoichiometric SiC and have received a surface coating. In the case of the filament referred to as SiC(1), the coating consists of a mixture of SiC + C (~ 3.6 $\mu$m thick),

0022–2461/84 $03.00 + .12  

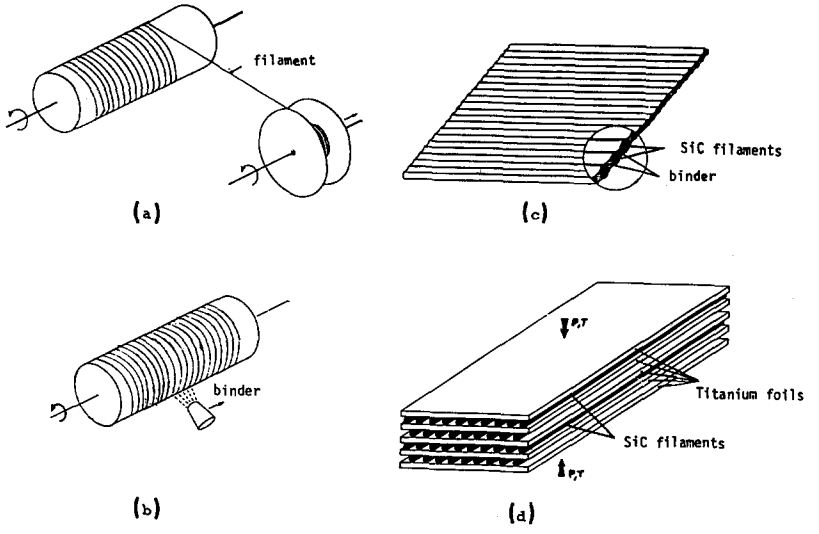


*Figure 1* Synthesis of unidirectional SiC/Ti composites by hot-pressing from titanium foils and SiC-filament monolayers.

while in that of the filament referred to as SiC(2), it is of almost pure pyrocarbon (~ 3.8 $\mu$m thick). It is to be noted that both are different, as far as the coating is concerned, from the SCS-type filament presently produced by AVCO [15, 16].

It has been established that the mean tensile stress of both SiC(1) and SiC(2) at room temperature (gauge length: 40 mm) is of the order of 4200 MPa and only 3000 MPa for the tungsten core SiC(3) filament [13].

The SiC/Ti or SiC/Ti–6Al–4V samples used for the FM chemical interaction experiments were prepared by hot-pressing at 850° C and under high vacuum ($10^{-5}$ to $10^{-6}$ torr), from unidirectional SiC-filament monolayers and titanium foils (50 or 100 $\mu$m thick) stacked together according to a given sequence as already described elsewhere (Fig. 1) [12]. The organic fugitive binder was carefully eliminated at 400 to 500° C under vacuum before temperature and uniaxial pressure were raised to 850° C and 90 to 180 MPa, respectively, for 20 to 30 min (Fig. 2).

The samples (80 mm x 80 mm x 0.8 to 1.8 mm; 4 to 9 filament layers; $V_f = 0.32$) were then cut, parallel to the filament direction, with a low-speed diamond saw, set inside silica glass tubes (contain-

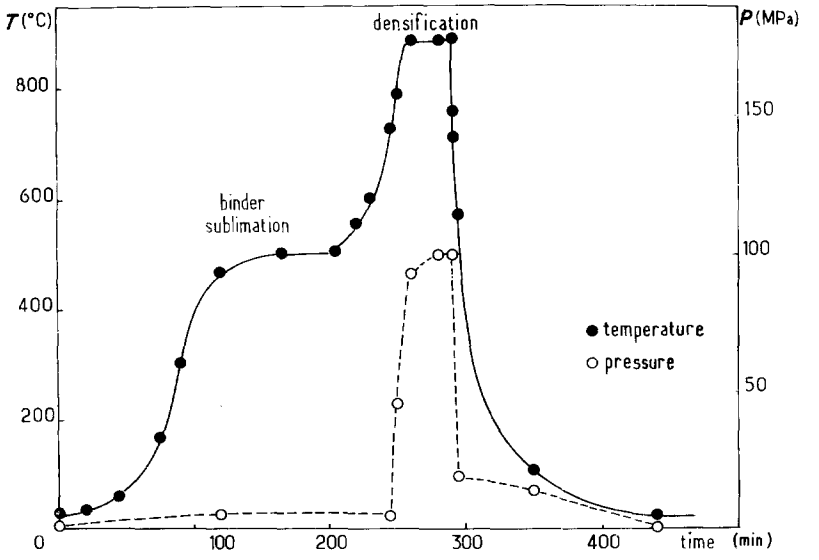


*Figure 2* Variation of temperature and applied uniaxial pressure during the synthesis of a SiC/Ti–6Al–4V composite.

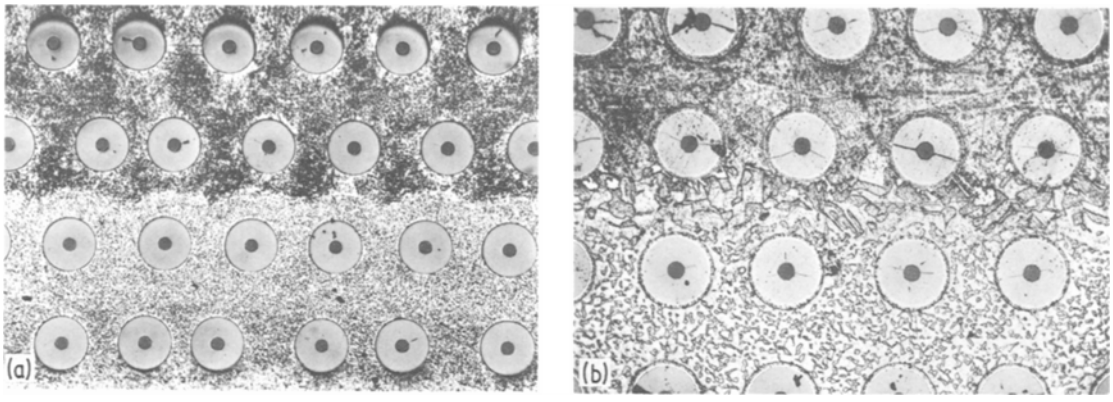

*Figure 3* Hybrid SiC/Ti and SiC/Ti–6Al–4V composites: (a) as-produced, × 70; (b) after annealing for 170 h at 900° C in vacuum-sealed tubes (view perpendicular to filament direction, after etching) × 100.

ing titanium powder as a getter) and sealed under high vacuum. They were annealed at a temperature ranging from 700 to 1100° C (temperature regulated at ± 1° C) for durations up to 300 h, cooled and analysed on carefully polished and etched cross-sections (silicon carbide paper 400, 15 and 1 μm diamond pastes, 50 nm alumina suspension, $HF + HNO_3 + H_2O$ etching mixture) (Fig. 3).

The FM interaction zones were studied by optical microscopy, SEM, X-ray electron microprobe (diameter ~ 1 μm), Auger electron microprobe (diameter ~ 200 nm) and X-ray diffraction. Their thicknesses were measured either under the optical microscope (averages of 50 to 80 measurements) or from the Auger line scans in a few cases.

## 2. Analysis of the FM interaction zones

In non-equilibrium metal matrix composites heated at high (and even medium) temperatures, diffusion phenomena result in an FM interaction layer growing radially around each fibre and exhibiting a brittle character when it becomes thick enough. The nature of this FM interaction layer is closely related to the corresponding phase diagram. It usually contains several compounds or/and solid solutions of the fibre and matrix elements. Its analysis can be rather accurately carried out, when its thickness is sufficiently large and the number of elements limited, by conventional X-ray electron microprobe techniques, as previously illustrated for B/Ti composites [12, 17, 18].

On the other hand, an accurate analysis of the FM interaction zone becomes more and more difficult and the results uncertain as the number of elements and thus the complexity of the system increase. This is particularly the case for both SiC/Ti and SiC/Ti–6Al–4V composites, as already emphasized by several investigators [1–10]. In the present work, the analysis of the FM interaction layer has been performed mainly by SEM and electron microscope techniques (the X-ray microprobe analysis is accurate, but its spatial resolution rather poor (of the order of 1 μm), whereas the Auger microprobe has a better spatial resolution (of the order of 200 nm diameter) but its use is limited to semiquantitative analysis). The interest of X-ray diffraction is limited owing to the small amount of material within the FM reaction layers, to the difficulty encounted in chemically extracting the fibres with their reaction products from the matrix, and finally to the fact that the FM reaction products are characterized by Debye–Scherrer patterns having most of their strongest lines overlapping.

The complexity of the FM reaction layers is illustrated in Figs. 4 to 6 for some of the samples which have been analysed. It clearly appears that the FM reaction layer contains several phases as already pointed out by the early investigators and as could be predicted from the phase diagram (a 1200° C isothermal section of the ternary Ti–Si–C phase diagram has been established by Brukl [19] (Fig. 7).

### 2.1. SiC/Ti composites

X-ray quantitative electron microprobe analyses performed on selected optically well-defined areas, for titanium and silicon, have shown that the main products of the FM interactions are:

1. the binary titanium carbide $TiC_{1-x}\square_x$ (with $0.14 < x < 0.44$);

2. a titanium silicide containing a small amount

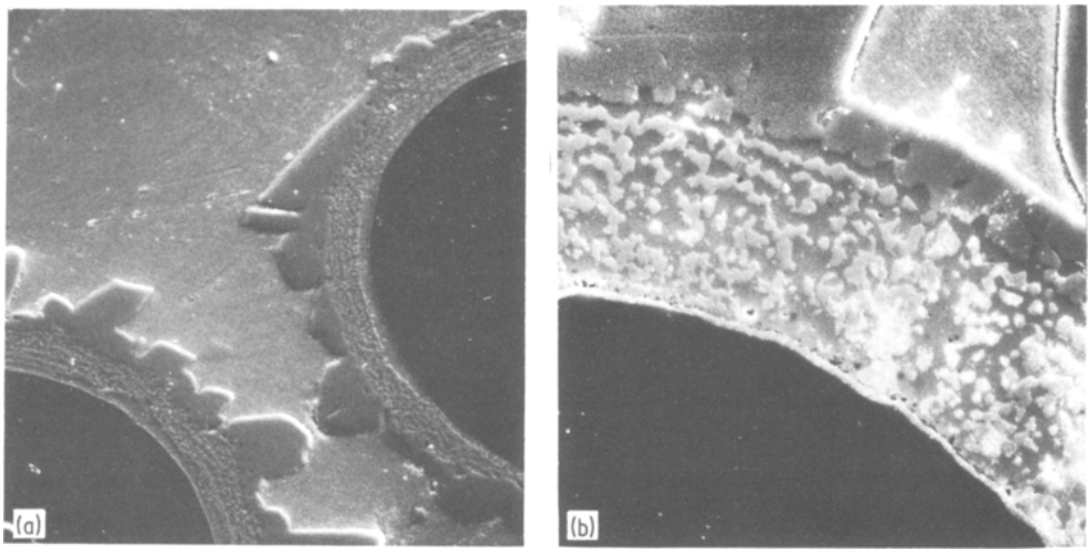


*Figure 4* SiC(1)/Ti composites annealed at 950° C: (a) for 96 h, × 1600; (b) for 300 h, × 600 (SEM micrographs after chemical etching).

of carbon $Ti_5Si_3$ (C) (Ti: 74.0; Si: 26.0 wt% as measured, compared to Ti: 73.975; Si: 26.025 wt% theoretical, carbon was detected but in too small an amount to be quantitatively analysed);

3. a ternary phase whose composition appears to be close to $Ti_3Si_{1,2}C_{2,3}$. According to Brukl [19], the maximum solubility of carbon in $Ti_5Si_3$ is only 8% and the formula of the ternary phase is close to $Ti_3Si_{1,31}C_{1,94}$. The ternary phase belongs to the class of the complex carbides characterized by octahedral $M_6C$ units; its crystal formula is $Ti_3SiC_2$, according to Jeitschko and Nowotny [20, 21].

In all cases, the most important part of the FM interaction zone is made of a binary mixture of titanium carbide $TiC_{1-x}\square_x$ and titanium silicide $Ti_5Si_3(C)$, as shown by the scanning electron micrographs, the X-ray and Auger line scans and quantitative analyses (Figs. 4 to 6, 8, 9). As already mentioned by House, the titanium carbide crystals tend to form concentric rings around the fibre (Figs. 5a, 6a) [10]. Within this binary subzone the

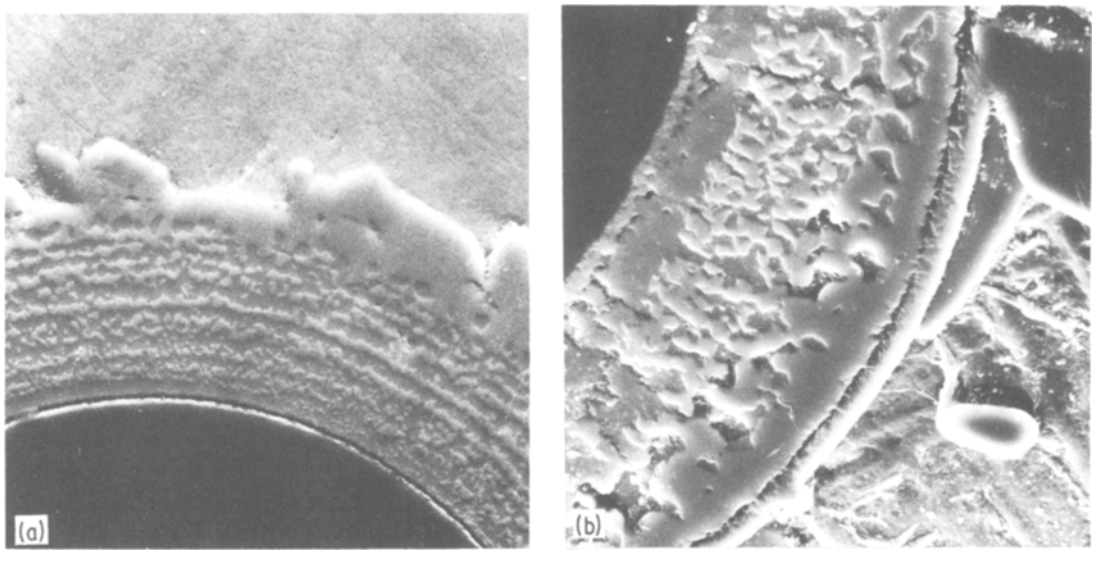


*Figure 5* SiC(2)/Ti composites annealed at 950° C: (a) for 196 h, × 1200; (b) for 265 h, × 1800 (SEM micrographs after chemical etching).

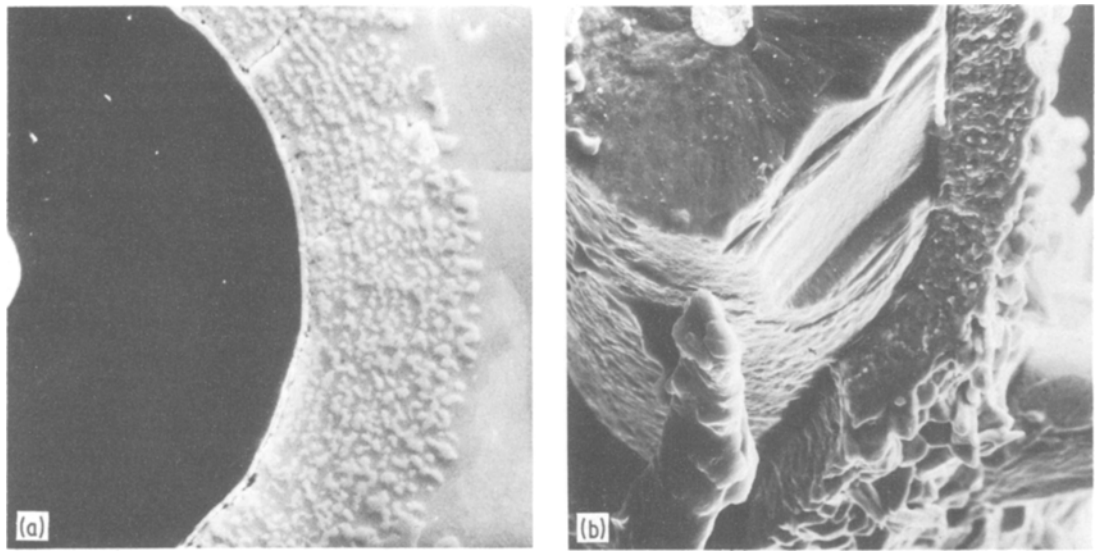


*Figure 6* SiC(3)/Ti composites annealed 290 h at 950° C: (a) polished and etched cross-section, × 1200; (b) filament and reaction products extracted from matrix, × 700.

relative amount of titanium carbide depends on the filament type: it seems higher for the two filaments having a surface coating containing elemental carbon (SiC(1) and SiC(2)) than for the uncoated stoichiometric SiC(3) filament.

The inner side of the binary $TiC_{1-x}\square_x$ + $Ti_5Si_3(C)$ subzone is separated from the surface filament by a layer of ternary phase. In a few cases this ternary phase layer was thick enough (see, for example, Fig. 4, for SiC(1) and Fig. 5b for SiC(2)) to be quantitatively analysed by X-ray electron microprobe. However, in most cases this layer was very thin and could only be observed by SEM and AES techniques. For the filaments which had received a carbon-based coating, the inner side of the binary subzone in contact with the ternary phase seems to be mainly $Ti_5Si_3(C)$, as shown in Fig. 5b for SiC(2).

The nature of the outer side of the binary subzone differs in the same manner according

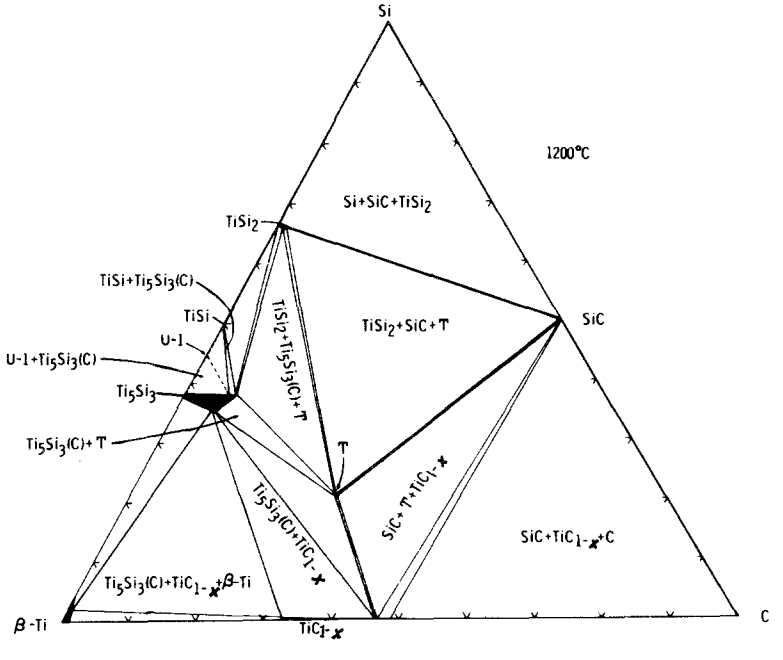


*Figure 7* Ti–Si–C ternary phase diagram: 1200° C section, according to Brukl [19].

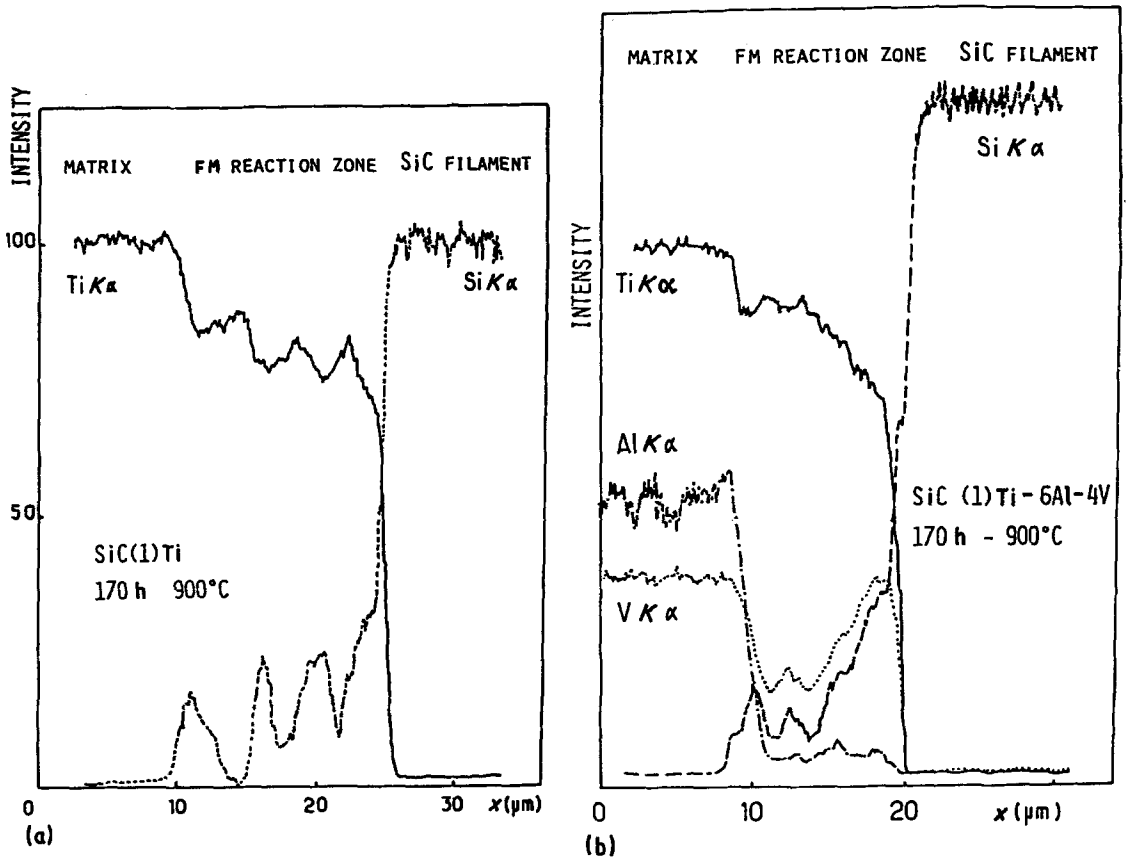


*Figure 8* X-ray line scans on cross-sections of (a) SiC(1)/Ti and (b) SiC(1)/Ti–6Al–4V composites annealed 170 h at 900° C. Note the difference in intensity scales for Si and Ti on the one hand and for Al and V on the other, in (b).

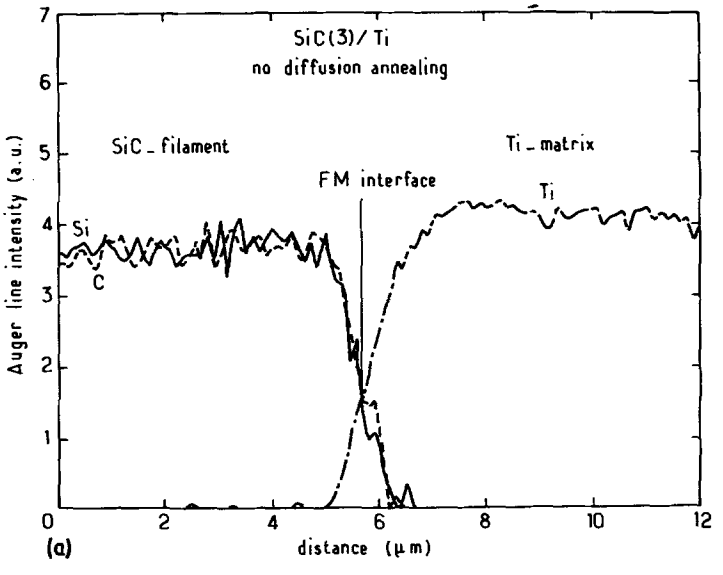


*Figure 9* Auger line scans on cross-sections of SiC/Ti composites: (a) SiC(3)/Ti as-produced (no diffusion annealing); (b) SiC(3)/Ti annealed 290 h at 950° C; (c) SiC(2)/Ti annealed 17 h at 950° C.

*Figure 9* Continued.

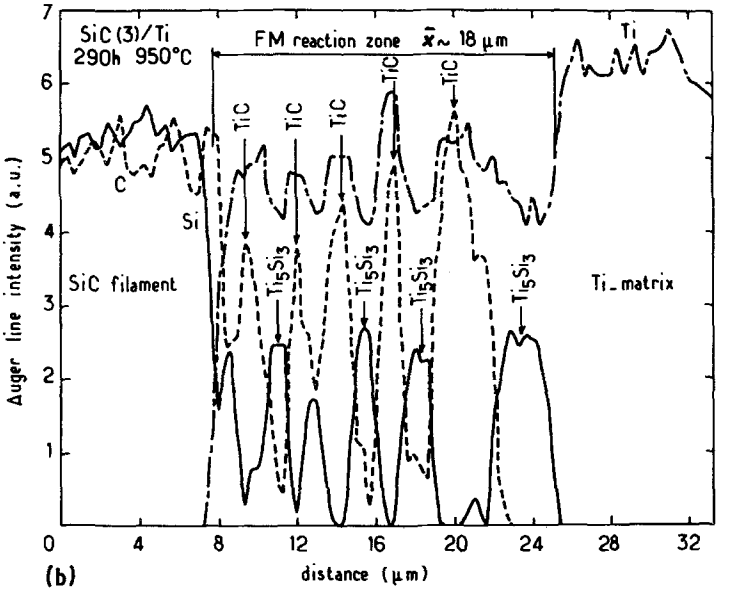


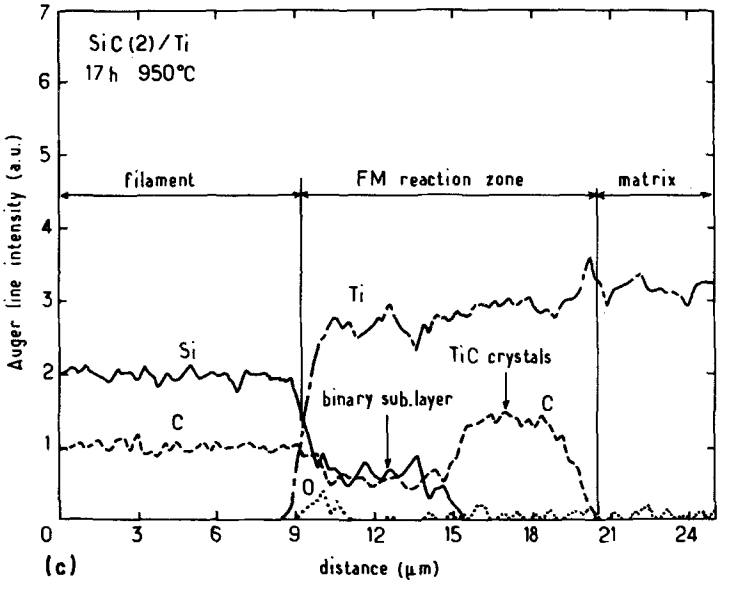


to the filament type. For both SiC(1) and SiC(2), it is essentially made of titanium carbide with large crystals having precipitated deeply into the titanium matrix, as shown in Figs. 4 and 5. On the other hand, for SiC(3) the outer side is made principally of $Ti_5Si_3$(C) (Fig. 6a).

## 2.2. SiC/Ti–6Al–4V composites

Although analysis becomes more difficult for a Ti–6Al–4V alloyed matrix, it appears that the main features of the SiC/Ti reaction zone are retained in SiC/Ti–6Al–4V composites. Three phases are still present and they are distributed in the FM reaction zone in a similar manner (Fig. 10).

The Auger line scans clearly show that the alloying elements do not markedly enter the FM reaction zone which remains principally made of combined titanium, silicon and carbon (Fig. 11). This is particularly true for aluminium, as already noted by House [10]. Such behaviour of the aluminium alloying element has also been observed for the related B/Ti–6Al–4V composites [12, 17, 18].

The main part of the FM reaction zone remains a binary $TiC_{1-x}\square_x + Ti_5Si_3$(C) type subzone. Its

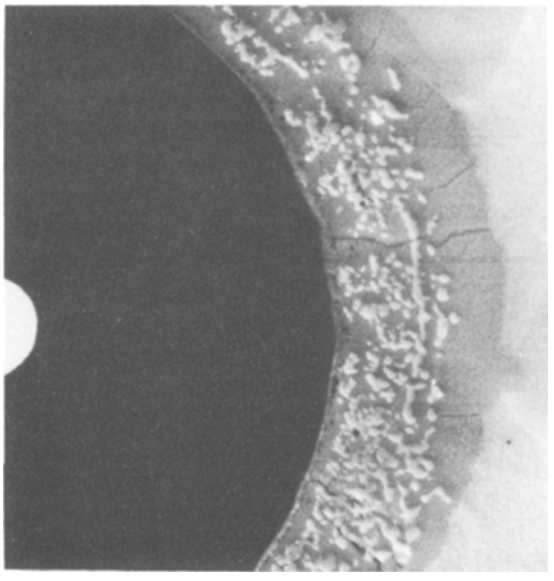

*Figure 10* SiC(3)/Ti–6Al–4V annealed 290 h at 950° C (SEM micrograph after etching), × 1000.

inner side, principally made of $Ti_5Si_3(C)$, is separated from the filament by a thin layer of $Ti_3SiC_2$-type ternary phase. Its outer side is principally composed of $TiC_{1-x}\square_x$ in the case of SiC(1) and SiC(2), and of $Ti_5Si_3(C)$ in the case of SiC(3) (Figs. 10 and 11).

## 2.3. Discussion

From the above analysis it appears that the main part of the well-developed FM reaction zones in SiC/Ti or SiC/Ti–6Al–4V composites annealed at 700 to 1100° C is a mixture of $TiC_{1-x}\square_x$ and $Ti_5Si_3(C)$, a result which confirms the conclusions of the early investigators [1, 4, 10]. This binary subzone is separated from the filament surface by a thin layer of a ternary phase (of the $Ti_3SiC_2$-type) which was also observed by Ratliff and Powell [1] in SiC/Ti diffusion couples (plan interfaces) but not detected by House [10] in fibrous samples.

The inner side of the binary subzone appears to be principally composed of $Ti_5Si_3(C)$ in contradiction to the conclusion of Ratliff and Powell [1] according to whom it could be essentially composed of titanium carbide. It should be noted that they are the only authors to support this point of view and that the SiC in their diffusion couples was not pure SiC but a mixture of SiC and elemental silicon (8.3 wt %).

The main difference between the behaviour of the filaments is found at the interface between the binary subzone and the metal matrix. For both filaments having received a carbon-based coating (SiC(1) and SiC(2)), the outer side of the binary subzone is mainly composed of titanium carbide, especially for SiC(2) (characterized by a rather thick coating of almost pure pyrocarbon) where large crystals have precipitated deeply within the titanium matrix. On the other hand, for the uncoated stoichiometric SiC(3) filament, the outer side is principally made of $Ti_5Si_3(C)$. This difference, which apparently has not been recognized up to now, is important because the well-faceted large titanium carbide crystals could act as severe stress concentrators.

Finally, when pure titanium is replaced by Ti–6Al–4V, the alloying elements (particularly

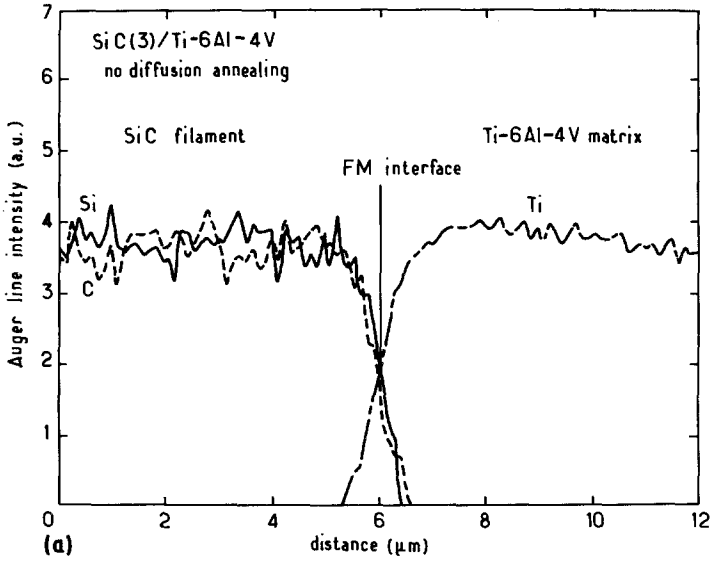


*Figure 11* Auger line scans on cross-sections of SiC/Ti–6Al–4V composites: (a) SiC(3)/Ti–6Al–4V as-produced (no diffusion annealing); (b) SiC(3)/Ti–6Al–4V annealed 290 h at 950° C; (c) SiC(2)/Ti–6Al–4V annealed 8 h at 950° C.

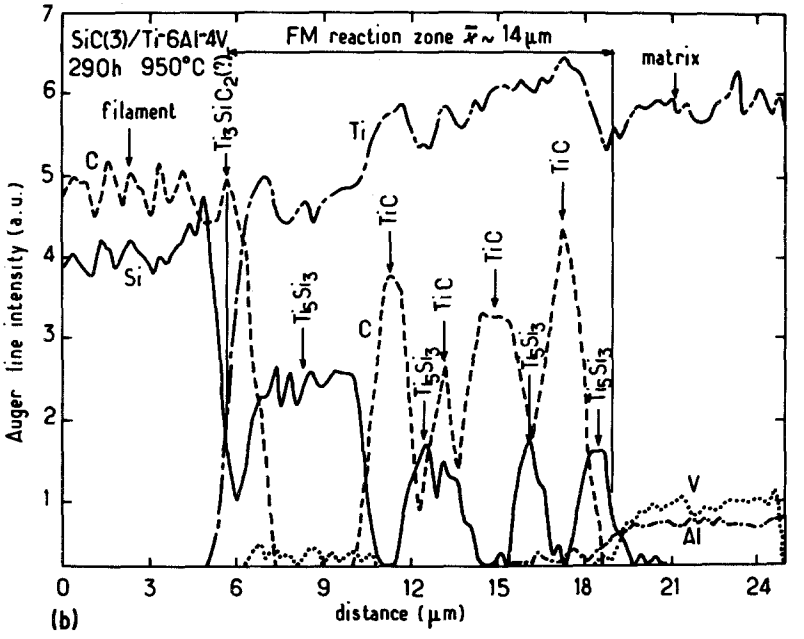


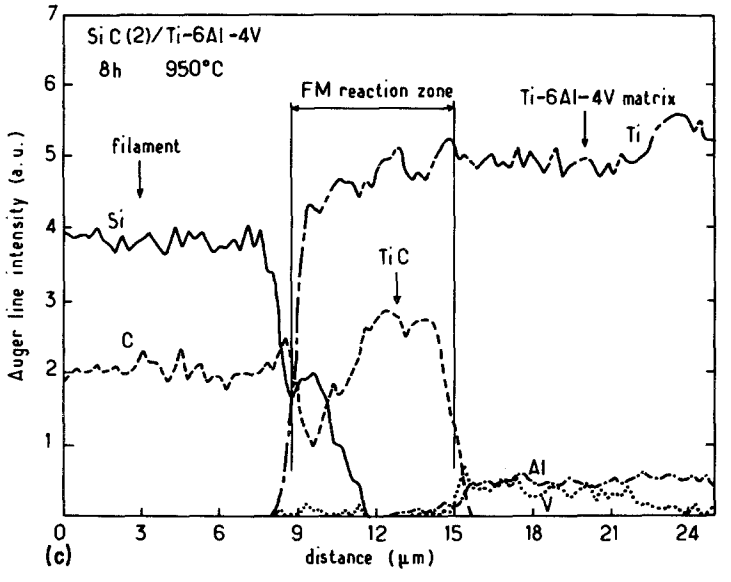


*Figure 11* Continued.

aluminium) do not significantly enter the FM reaction zone and are rejected in the matrix. From this result and as already suggested by House [10], it could be of interest to use Ti–Al alloys with a higher aluminium concentration, to slow down the FM reaction rate.

## 3. Kinetics of growth of the FM reaction zone

### 3.1. Measurements of the FM reaction zone thickness

In such materials, the growth kinetics of the FM reaction zone is usually studied from thickness measurements performed under the optical microscope on polished sections cut perpendicular to the filament direction.

An important difficulty arises from the fact that in SiC/Ti or SiC/Ti–6Al–4V composites, the FM reaction zone usually does not have a regular contour on the matrix side. This is particularly true for both SiC(1) and SiC(2) based composites where large titanium carbide crystals have grown in front of the compact reaction zone sublayers (Figs. 4, 5). Since such protuberant crystals remain limited in number and are observed only in some samples, it was decided to use the main thickness

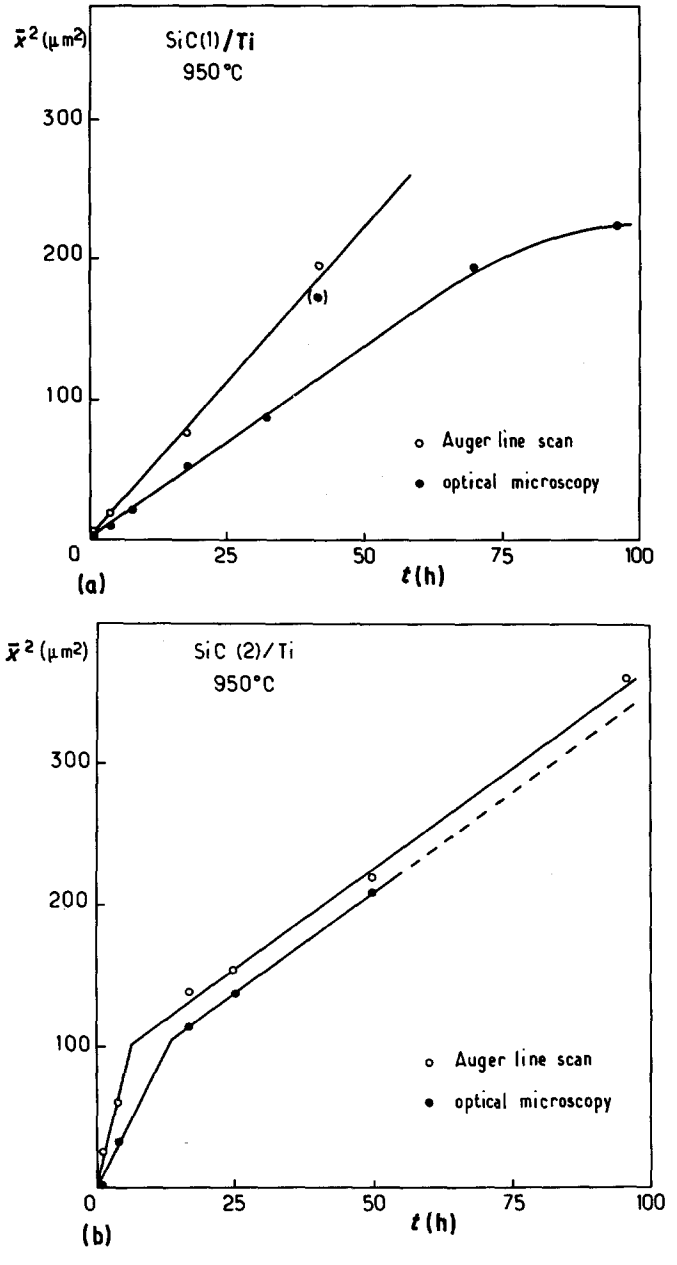


*Figure 12* Comparison between the FM reaction zone thicknesses measured under an optical microscope or deduced from Auger line scans: (a) SiC(1)/Ti annealed at 950° C; (b) SiC(2)/Ti annealed at 950° C.

($\bar{x}$) of the compact layers as a basis for the kinetics study. Such a choice has already been investigated and discussed in the case of B/Ti composites where a compact layer of titanium diboride is often surrounded by acicular TiB crystals in the FM reaction zone [11, 12, 17, 18, 22].

The mean thickness, $\bar{x}$, was in each case calculated from 50 to 80 individual measurements performed under the optical microscope. In order to establish whether or not the optical contour to the true limit of the FM reaction zone on the matrix side (i.e. the point in the matrix where both the carbon and silicon concentrations become almost zero), the data were compared to those deduced from the carbon and silicon Auger line scans. Although the latter were more limited in number than the former, an acceptable agreement was found (as far as the limitations of both techniques allow) (Fig. 12). Therefore, all thickness data reported in the following sections were determined by optical microscopy.

## 3.2. Kinetics of growth

The thickness of the FM reaction zone, $\bar{x}$, in-

TABLE I Values of $k$ ($10^6$ cm $sec^{-1/2}$) for various composites made of silicon carbide filaments and titanium-based matrices

| $\theta$(° C) | Ti | | | | Ti–6Al–4V | | |
|---|---|---|---|---|---|---|---|
| | SiC(1) | SiC(2) | | SiC(3) | SiC(1) | SiC(2) | SiC(3) |
| | | Stage I | Stage II | | | | |
| 700 | 0.21 | 0.18 | – | 0.07 | 0.094 | 0.11 | 0.06 |
| 750 | – | 0.47 | – | 0.206 | – | 0.18 | 0.11 |
| 800 | 0.69 | 0.833 | – | 0.69 | 0.39 | 0.45 | 0.27 |
| 850 | 1.26 | 1.37 | – | 0.74 | 0.7 | 0.77 | 0.49 |
| 900 | 1.83 | – | 1.51 | 1.05 | 1.27 | 1.20 | 0.99 |
| 950 | 2.64 | 4.4 | 2.92 | 2.99 | 2.18 | 2.24 | 1.59 |
| 1000 | 4.75 | 6.92 | 4.1 | 4.30 | 3.47 | 3.22 | 2.48 |
| 1100 | – | – | 10.54 | – | – | 7.71 | – |

creases linearly with the square root of the annealing time, $t$, at a given temperature, at least in a first approximation and if the FM reaction zone is not too thick:

$$\bar{x} = kt^{1/2} \qquad (\text{or } \bar{x}^2 = k^2 t) \qquad (1)$$

where $k$ is a material constant ($k^2$ has the dimension of a diffusion coefficient $L^2T^{-1}$), as shown in Figs. 13 to 15. The values of $k$ calculated from the slopes of the $x^2 = f(t)$ straight lines, are given in Table I for the various filament/matrix associations.

The thermal variations of $k$ follow an Arrhenius law in the 700 to 1100° C temperature range:

$$k = k_0 \exp\left(-\frac{Q}{2RT}\right) \quad \text{or } \ln k = \ln k_0 - \frac{Q}{2RT} \qquad (2)$$

where $k_0$ and $Q$ (the activation energy) are material constants, $T$ the absolute temperature and $R$ the gas constant ($R = 1.9872$ cal $K^{-1}$), as shown in Fig. 16. The values of $k_0$ and $Q$ are given in Table II.

## 3.3. Discussion

The experimental results show that growth of the FM reaction zone is mainly controlled by diffusion phenomena, as previously well established for the related B/Ti composites [11, 12, 17, 18]. Thus the rate of formation of the FM reaction zones increases very rapidly with increasing temperature. As an example, from the values of $k$ given in Table I it appears that a 1 $\mu$m thick FM reaction zone is achieved in about 570 h at 700° C but in only 9 min at 1000° C for SiC(3)/unalloyed titanium composites. This feature explains the importance of an accurate control of temperature and duration during the high temperature step of the synthesis procedure of the materials (Fig. 2).

Growth of the FM reaction zone consumes both filament and matrix, as already mentioned by House [10]. As an example, the filament diameter undergoes a 16% decrease (from 140 to 118 $\mu$m) after 340 h annealing at 950° C in SiC(2)/Ti composites. Simultaneously, the filament surface through which diffusion occurs, falls by 32%. Thus in SiC/Ti composites diffusion is not a one-way phenomenon: both carbon and silicon on the one hand and titanium on the other diffuse in opposite directions through the FM reaction zone (in contrast to the related B/Ti composites where diffusion mainly occurs from the filaments towards the matrix). Therefore the vacancy flux through the FM reaction zone (as well as pore precipitation near the interface and the associated strength weakening effects) must be lower in SiC/Ti than in B/Ti composites. Finally, the thickness data correction suggested by Thebault [23, 24] to take into account the cylindrical

TABLE II Values of $Q$ and $k_0$ for various composites made of silicon carbide filaments and titanium-based matrices

| | Ti | | Ti–6Al–4V | |
|---|---|---|---|---|
| | $Q$(cal $mol^{-1}$) | $k_0$(cm $sec^{-1/2}$) | $Q$(cal $mol^{-1}$) | $k_0$(cm $sec^{-1/2}$) |
| SiC(1) | 52 400 | 0.37 | 59 260 | 0.41 |
| SiC(2) | – | – | 58 180 | 0.31 |
| Stage I | 56 600 | 1 | | |
| Stage II | 63 000 | 1.30 | | |

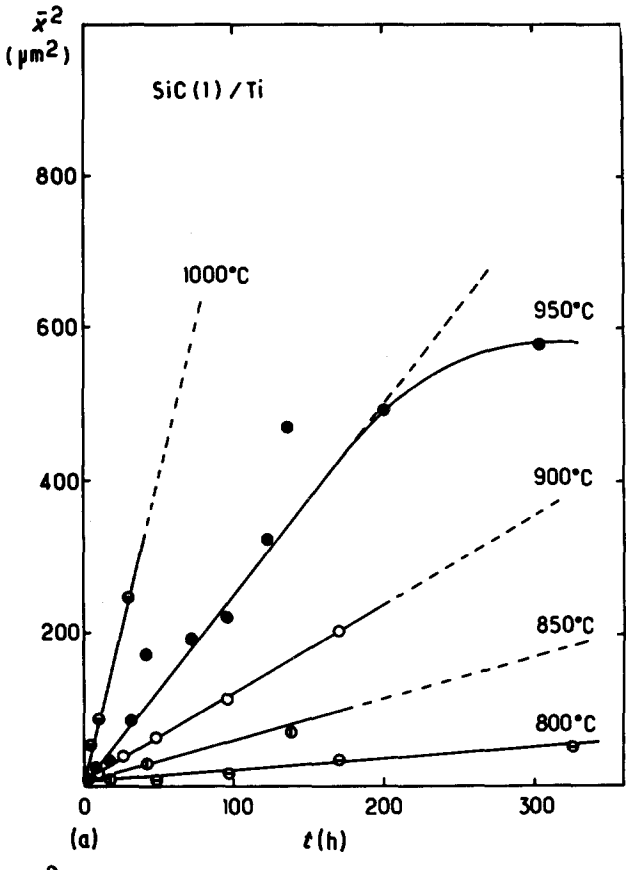


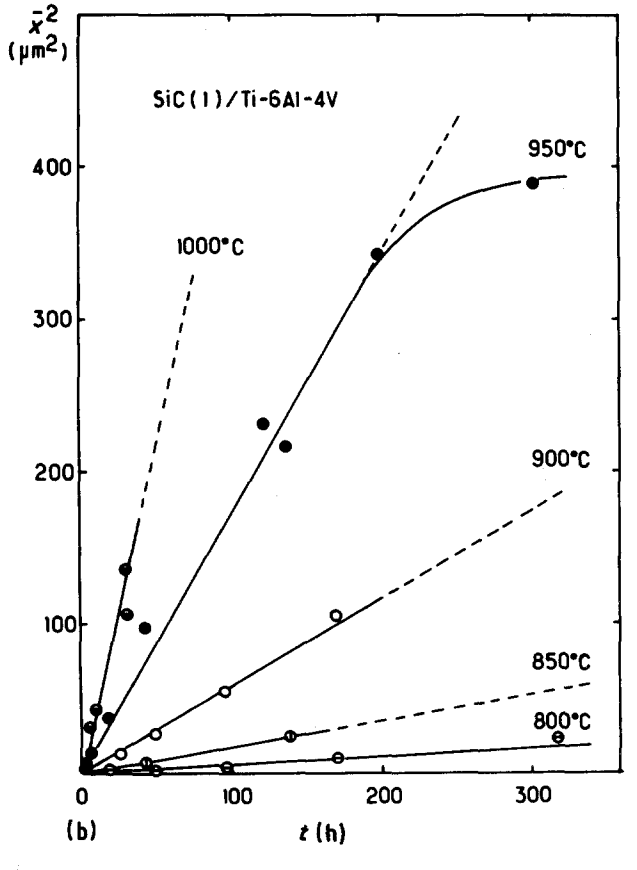


*Figure 13* $\bar{x}^2 = f(t)$ curves for (a) SiC(1)/Ti and (b) SiC(1)/Ti–6Al–4V composites annealed at various temperatures.

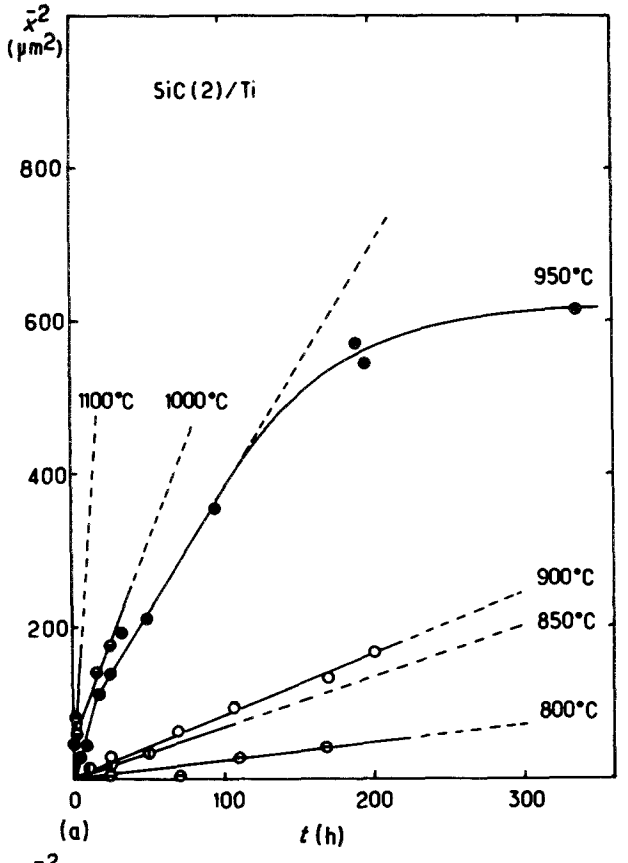


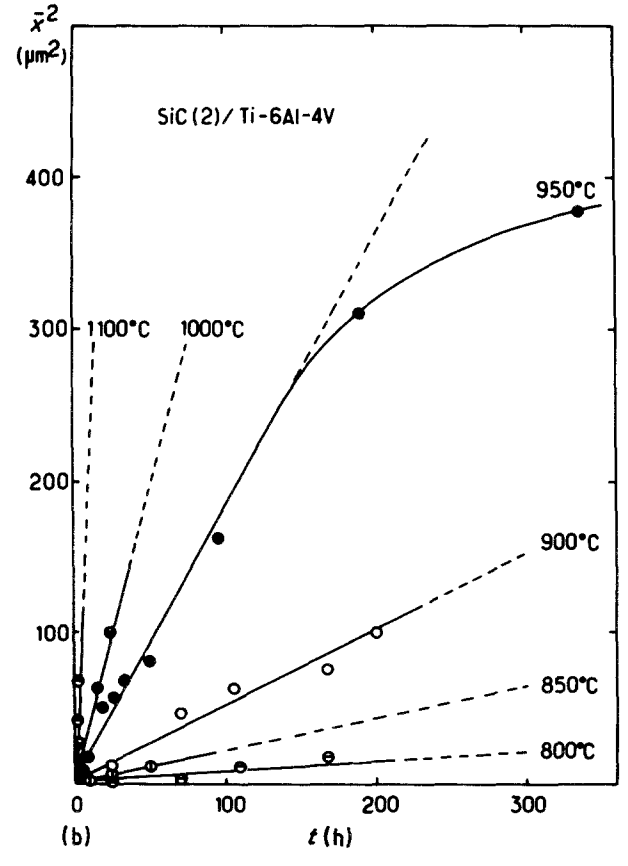


*Figure 14* $\bar{x}^2 = f(t)$ curves for (a) SiC(2)/Ti and (b) SiC(2)/Ti–6Al–4V composites annealed at various temperatures.

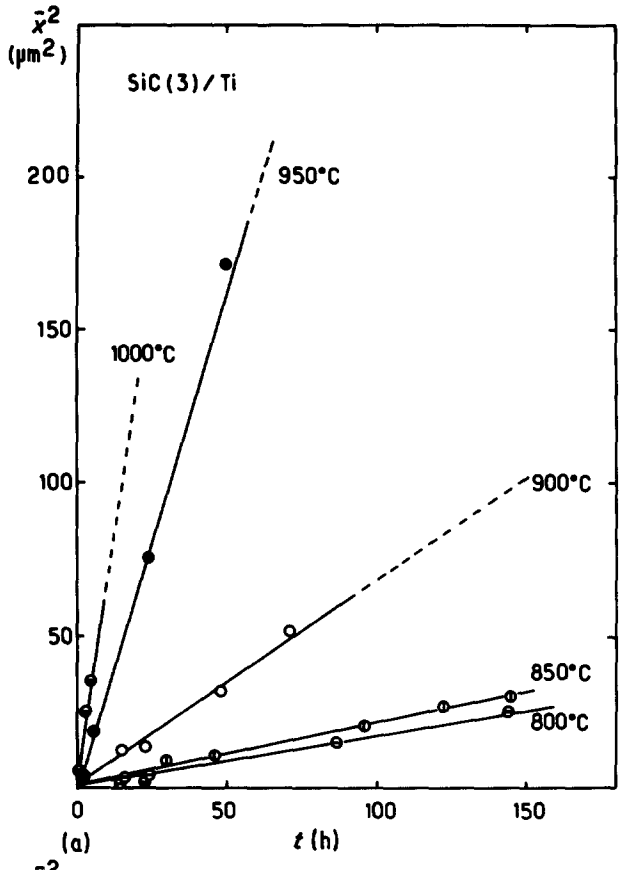


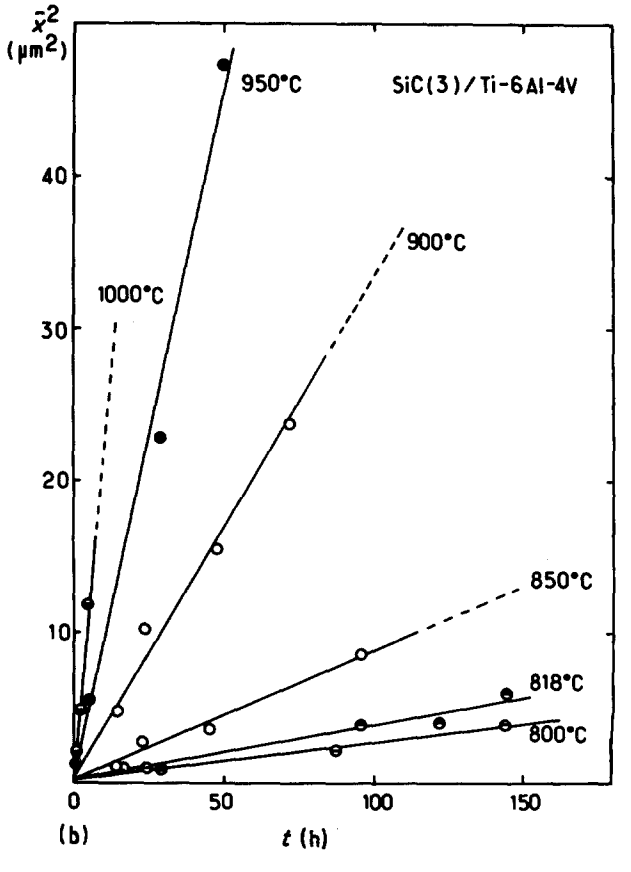


*Figure 15* $\bar{x}^2 = f(t)$ curves for (a) SiC(3)/Ti and (b) SiC(3)/Ti–6Al–4V composites annealed at various temperatures.

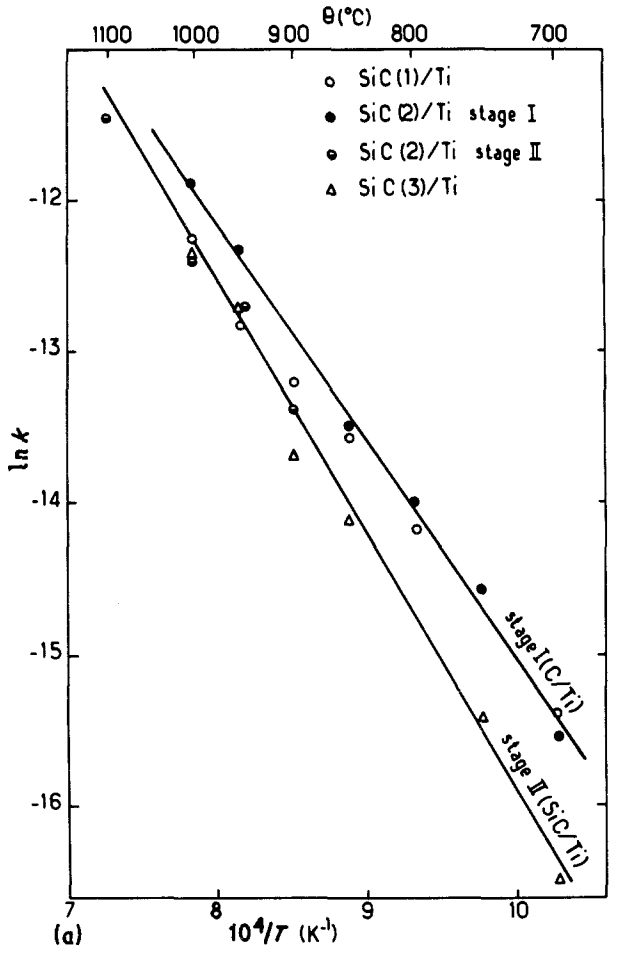


*Figure 16* $\ln k = f(1/T)$ Arrhenius plot for (a) SiC/Ti and (b) SiC/Ti–6Al–4V composites annealed at temperature ranging from 700 to 1100° C.

geometry of the diffusion interface in B/Ti composites (with respect to diffusion couples with plan interface), could not be applied here since it assumes that the diffusion interface area (and thus the filament diameter) remains constant.

As shown in Figs. 13 to 15 and 17, the FM reaction zone thickness data cannot be fitted to a single $\bar{x}^2 = k^2 t$ straight line within the whole $t$-axis and for all filament types. Two types of deviation are observed:

1. for short annealing times and essentially for SiC(2) filaments (Figs. 12b, 14a and 17); and/or

2. for long annealing durations, i.e. thick FM reaction zones (for both SiC(1) and SiC(2) (as well as presumably for SiC(3)) (Figs. 13, 14 and 17)).

It must be underlined that only the former is of practical interest since the latter occurs in composites where the filaments are so corroded and the FM reaction zones so thick that the strength must be extremely weak and the physical integrity of the materials questionable:

1. For short annealing times (e.g. $t < 100$ to 150 h at 950° C for unalloyed matrices), the thickness data for SiC(2) filaments can be fitted to two $\bar{x}^2 = k^2 t$ straight lines (stages I and II) having different slopes (Figs. 12b, 14a and 17) suggesting that two diffusion mechanisms are successively involved. In stage I the value of $k$ is much higher than in stage II ($k = 4.4 \times 10^{-6}$ and $2.9 \times 10^{-6}$ cm $\sec^{-1/2}$, respectively, at 950° C and for unalloyed titanium). On the basis of the nature of the coating which has been applied to SiC(2) filaments, it was thought that stage I could be associated with interactions between pyrocarbon and titanium (with formation of titanium carbide) whereas stage II could be related to those involving stoichiometric SiC itself when the pyrocarbon coating is totally consumed (with thus formation of more complex reaction products). In order to ascertain this hypothesis,

*Figure 16* Continued.

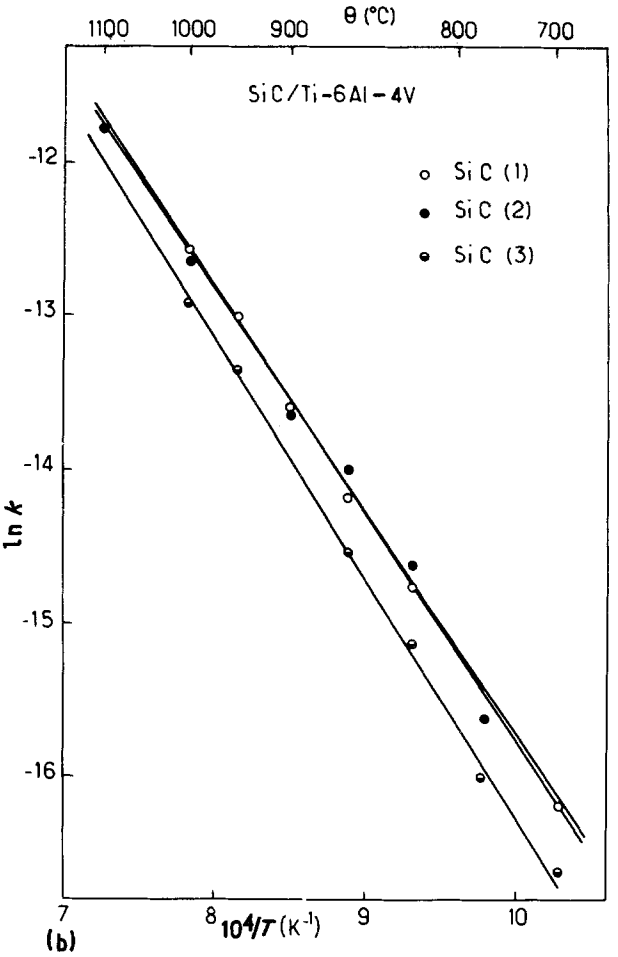


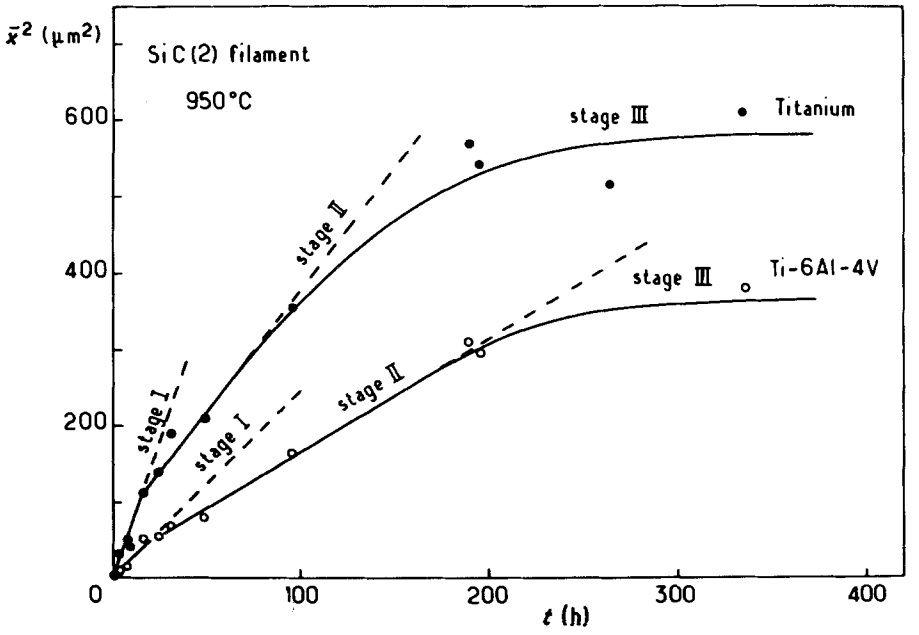


*Figure 17* $\bar{x}^2 = f(t)$ curves for SiC(2)/Ti and SiC(2)/Ti–6Al–4V composites showing the occurrence of three different stages in the kinetics of growth of the FM reaction zone.

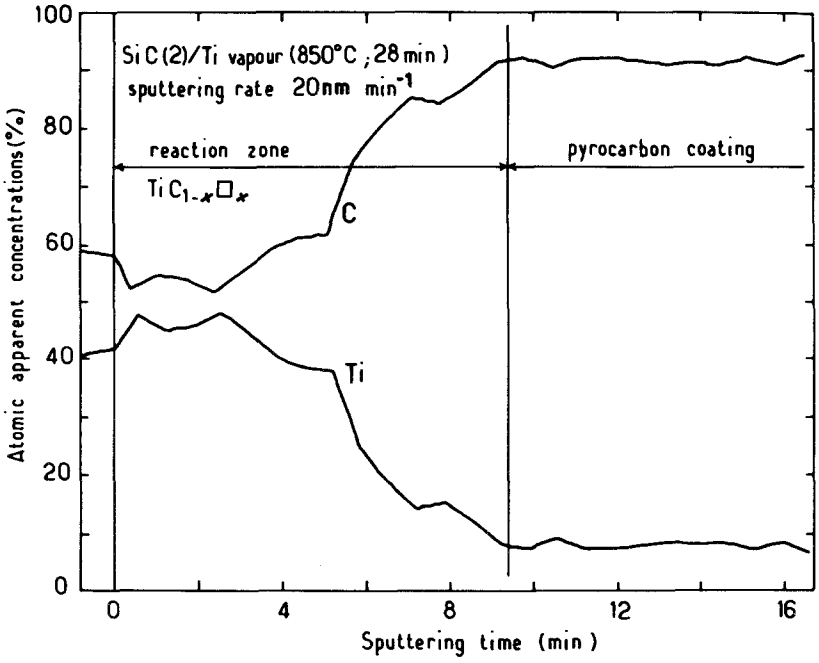


*Figure 18* AES depth profiling from the surface of an SiC(2) filament reacted at 850° C (28 min) with titanium vapour inside a vacuum-sealed silica glass tube (the sputtering rate is given for tantalum oxide used as a standard).

bundles of as-received SiC(2) filaments were sealed under vacuum in silica glass tubes containing at one end a small amount of titanium powder and then annealed for short times at 850° C. Under such conditions, titanium is transported through the vapour phase from the powder sink to the filament surfaces where a controlled chemical reaction, similar to that occurring in solid state within SiC/Ti composites, takes place. AES analysis of the annealed filaments shows that the only reaction product is indeed titanium carbide (Fig. 18). Therefore, it appears to be established that stage I, which is observed for SiC(2) but not for SiC(3), must be related to the interactions between titanium and the pyrocarbon coating. From a practical point of view it means that a coating made of almost pure pyrocarbon significantly increases the chemical reactivity of SiC filaments with respect to metals.

2. For long annealing times (e.g. $t > 100$ h at 950° C for unalloyed titanium), the kinetics of growth of the FM reaction zone no longer follow a parabolic $\bar{x}^2 = k^2 t$ diffusion law (stage III), the measured thickness values being much lower than those extrapolated from the stage II $\bar{x}^2 = k^2 t$ straight line (Figs. 13, 14 and 17). Although no definite interpretation can yet be given to this deviation, several hypotheses may be formulated: (a) in such very thick reaction zones, one of the reaction product sublayers could become, at least partly, disconnected from the others (due to pore precipitation) thus lowering the diffusion fluxes; (b) as reaction zone thickness increases each filament is progressively consumed, the surface through which diffusion takes place becoming smaller and smaller; and (c) the matrix becomes saturated in both silicon and carbon. Points (b) and (c) are directly related to the fact that diffusion phenomena in a fibrous composite material are quite different from those occurring in a diffusion couple of infinite length with a plane interface. In a composite material, distances between adjacent filaments can be very short, especially when the filament volume fraction $V_f$ is high (Fig. 3), and furthermore the interfaces through which diffusion takes place are cylindrical. Therefore, if the usual diffusion laws still describe quite well the kinetics of growth of FM reaction zones of limited thickness, they could become inappropriate for extended FM reaction zones. In this direction, kinetics of growth of the FM reaction zone at a given temperature must depend on filament interspacing, i.e. on $V_f$. Thickness data corresponding to two types of composites prepared and annealed under the same conditions, but characterized by different

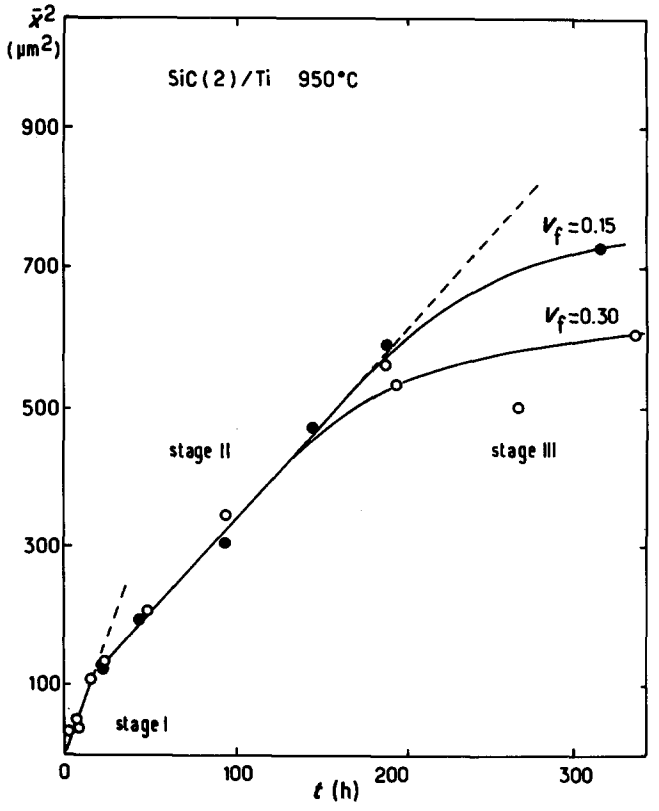


*Figure 19* $\bar{x}^2 = f(t)$ curves for SiC(2)/Ti composites annealed at 950° C and characterized by two different $V_f$ values.

$V_f$ values (0.15 and 0.30) seem to support this assumption, as shown in Fig. 19. A transition from stage II to stage III seems to occur earlier in the sample where the filament interspacing is the shortest (i.e. for $V_f = 0.30$). In such a material, saturation of the matrix with diffusing elements could be more easily achieved.

The above discussion gives a basis for the analysis of the Arrhenius plots shown in Fig. 16. For the unalloyed matrix, the data can be fitted in with two different Arrhenius straight lines: one (stage II) is assumed to be related to diffusion between stoichiometric SiC and titanium and the other one (stage I) to that between pyrocarbon and titanium (stage I) (Fig. 16a). For SiC(3)/Ti composites, all data points are well aligned along the former (since the SiC(3) filament is homogeneously made of stoichiometric SiC). For SiC(2)/Ti composites, the data points are accounted for either by the stage I straight line when the pyrocarbon coating is not totally consumed, or by the stage II straight line in the other case. For SiC(1)/Ti composites, the occurrence of two different growth kinetics was not clearly apparent from the $\bar{x}^2 = k^2 t$ curves (Fig. 13a). However, the Arrhenius plot suggests that weak interactions ($\theta < 850°$ C) could also be mainly controlled by a stage I mechanism and strong interactions ($\theta > 850°$ C) by a stage II mechanism. For the alloyed matrix, the FM reaction zone thicknesses are much weaker and the occurrence of two stages for the coated filaments still less apparent (Figs. 13b, 14b and 15b). As a result, the data have been accounted for on the basis of single $\bar{x}^2 = k^2 t$ straight lines for the three filament types. In fact, the Arrhenius plots shown in Fig. 16b could be more accurately analysed as those corresponding to the unalloyed matrix (Fig. 16a). SiC/Ti composites are usually prepared at about 850° C and utilized at a still lower temperature. Thus, under such conditions, the above analysis clearly shows that, from a practical point of view, it is the SiC(3) filament, made of stoichiometric SiC, which exhibits the highest chemical compatibility with titanium-based matrices. The filaments which have received a carbon-based coating appear to be characterized by higher reaction rates (related to formation of titanium carbide) under the conditions of synthesis and use of such materials ($\theta < 850°$ C, limited FM reaction zone thicknesses).

At a given temperature, the growth rate of the

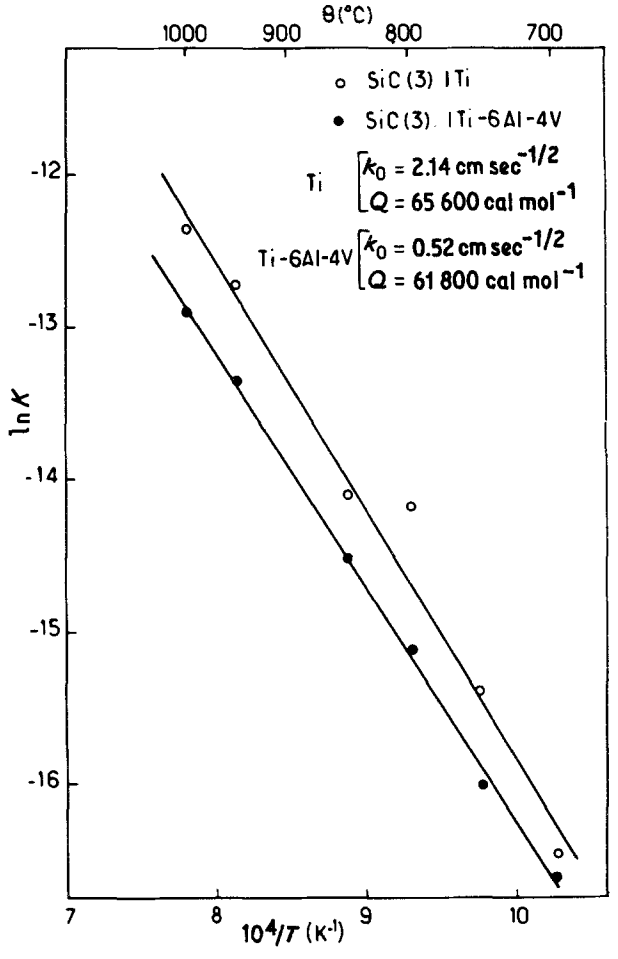


*Figure 20* $\ln k = f(1/T)$ Arrhenius plots for SiC(3)/Ti and SiC(3)/Ti–6Al–4V composites annealed at temperatures ranging from 700 to 1100° C.

FM reaction zone is lower for the alloyed Ti–6Al–4V matrix than for unalloyed titanium, as illustrated in Fig. 20 for SiC(3) filaments. Such an increase in chemical compatibility due to alloying elements has been mentioned previously for B/Ti composites: vanadium was found to form a ternary phase ($Ti_{1-x}V_xB_2$) with titanium whereas aluminium appeared to be rejected in front of the FM interface where it piled up [11, 12, 17, 18]. Although an accurate analysis of vanadium and aluminium is difficult in the more complex SiC/Ti–6Al–4V reaction zones, the X-ray and Auger line scans given in Figs. 8b and 11 strongly suggest that similar phenomena could also take place here. As mentioned by House [10], aluminium which does not seem to be present in the FM reaction zone (whereas vanadium is present in small amounts in $Ti_5Si_3(C)$) could play the most important role in the mechanism responsible for the reaction rate decrease.

Finally, the chemical reactivity of SiC filaments, with respect to both titanium and Ti–6Al–4V alloy, appears to be lower than that of uncoated boron filaments but similar to that of boron carbide coated boron filaments (on the basis of thickness measurements limited to the compact sublayers), in the temperature range of interest in the synthesis and use of such materials ($\theta < 850°$ C), as shown in Fig. 21. Therefore, the main interest of SiC compared to $B(B_4C)$ filaments seems to lie in their capability to retain an important percentage of their room temperature strength at high temperature, rather than in a chemical compatibility advantage (Table III).

## 4. Tentative models for the F/M interactions in SiC/Ti composites

On the basis of the above analyses, tentative models could be suggested to take into account the main features of the FM interactions in SiC/Ti composites.

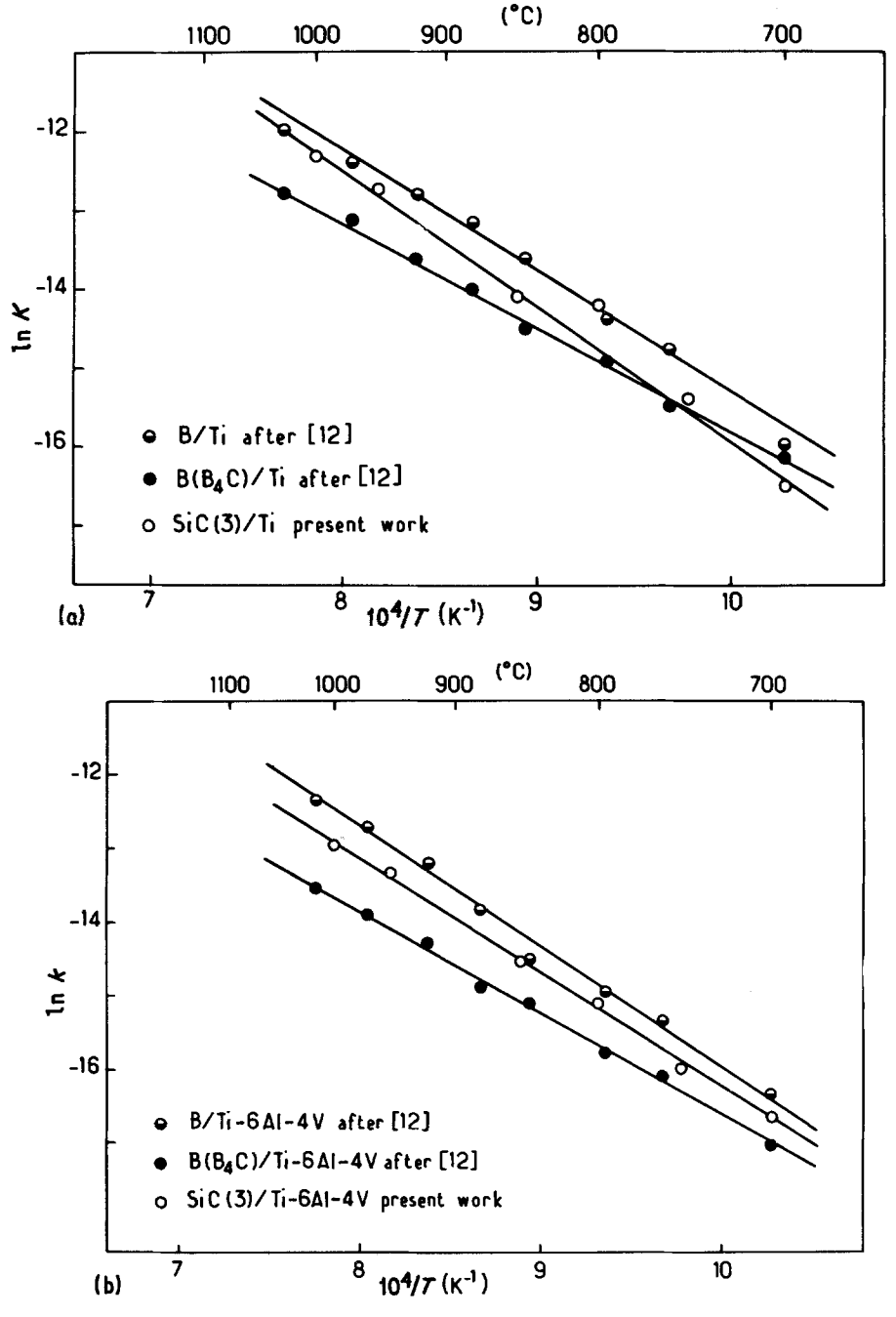


*Figure 21* Comparison of the chemical reactivity of B, $B(B_4C)$ and SiC filaments titanium-based matrices: (a) unalloyed titanium and (b) Ti–6Al–4V alloy. Data for B and $B(B_4C)$ filaments have been corrected according to Thebault [24].

TABLE III Values of $Q$ and $k_0$ for various composites made of boron and silicon carbide filaments and titanium-based matrices

| | Ti | | Ti–6Al–4V | |
|---|---|---|---|---|
| | $Q$(cal mol$^{-1}$) | $k_0$ (cm sec$^{-1/2}$) | $Q$(cal mol$^{-1}$) | $k_0$ (cm sec$^{-1/2}$) |
| B | 61 700 | 1.17 | 63 400 | 1.06 |
| $B(B_4C)$ | 53 100 | 0.09 | 54 400 | 0.06 |
| SiC(3) | 61 200 | 2.14 | 62 700 | 0.52 |

Values have been corrected by Thebault [24] for B, $B(B_4C)$.

### 4.1. Uncoated stoichiometric SiC filaments

In the first step, the interactions between SiC filaments and titanium could result in the formation of the ternary phase $Ti_3SiC_2$. Since the C/Si atomic ratio in $Ti_3SiC_2$ (i.e. C/Si = 2) is higher than in SiC (C/Si = 1), a silicide containing a small amount of carbon, $Ti_5Si_3C_x$, should be formed simultaneously. Although $TiSi_2$ could be in equilibrium simultaneously with SiC and $Ti_3SiC_2$, according to the ternary phase diagram section proposed by Brukl [19], its occurrence in significant amounts in the FM reaction zone was not detected either in the present work or in a similar study by House (Fig. 7) [10].

In the second step, the silicide $Ti_5Si_3(C)$ sublayer grows by interdiffusion of both silicon and carbon from filament to matrix and of titanium in the opposite direction. When $Ti_5Si_3(C)$ becomes sufficiently supersatured with respect to carbon, titanium carbide precipitates giving rise to concentric shells of $TiC_{1-x}\square_x$ crystals in a silicide matrix, as if waves of TiC were propagating through the FM reaction zone (Figs. 5a and 6a).

This model is different from that suggested by Ratliff and Powell [1]. According to these authors, the first step in SiC/Ti interaction could be the simultaneous formation of $Ti_5Si_3(C)$ and $TiC_{1-x}\square_x$. Since silicon was assumed to be the most mobile species, titanium carbide was located near the filament surface (whereas in both the present work and that of House [10] the inner side of the binary sublayer was found to be preferentially made of $Ti_5Si_3(C)$). When titanium carbide adjacent to the filament surface becomes sufficiently supersaturated with respect to both silicon and carbon, the ternary $Ti_3SiC_2$ phase was thought to be formed. According to Ratliff and Powell, the delayed deformation of $Ti_3SiC_2$ could be responsible for a modification of the growth rate of the FM reaction zone which they reported in the $\bar{x} = kt^{1/2}$ curves. More diffusion experiments on well prepared and characterized diffusion couples would be necessary to choose between the two models.

### 4.2. Pyrocarbon-coated SiC-filaments

For SiC(2) filaments, the first step in the FM interactions is the formation of $TiC_{1-x}\square_x$ (Figs. 5, 9 and 11). When all the pyrocarbon coating has been consumed, diffusion through titanium carbide (characterized by a wide homogeneity range) brings titanium atoms into contact with SiC and the reaction mechanism discussed above can take place. As a result, the binary $Ti_5Si_3(C) + TiC_{1-x}\square_x$ sublayer remains surrounded, on the matrix side, by a shell of large titanium crystals initially formed (Figs. 5 and 9).

Finally for SiC(1) filaments which have received a SiC + C coating, growth of the FM reaction zone could obey a hybrid mechanism.


## Acknowledgements

The authors wish to thank AVCO, SEP and SNPE for filament supply. This work was partly supported by CNRS (ATP-contract).


## References


1. J. L. RATLIFF and G. W. POWELL, Research on Diffusion in Multiphase Ternary systems: Reaction Diffusion in the Ti/SiC and Ti–6Al–4V/SiC Systems, AFML Techn. Report 70-42, 1970, US Department of Commerce, Nat. Tech. Inf. Serv. Springfield, Va.
2. M. B. CHAMBERLAIN, *Thin Solid Films* **72** (1980) 305.
3. J. A. SNIDE, Compatibility of Vapor Deposited B, SiC and $TiB_2$ Filaments with Several Titanium Matrices, AFML Tech. Report 67-354, US Department of Commerce, Nat. Tech. Inf. Serv. Springfield, Va.
4. J. A. SNIDE, F. A. ASHDOWN and J. R. MYERS, *Fibre Sci. Technol.* 5 (1972) 61.
5. G. ZIEGLER, H. J. DUDEK and W. BUNK, *Leichtmetalltag* 7 (1981) 204.
6. G. ZIEGLER and H. J. DUDEK, *Microchimica Acta (Wien) Suppl.* 8 (1979) 421.
7. E. P. ZIRONI and H. POPPA, *J. Mater. Sci.* **16** (1981) 3115.
8. M. KH. SHORSHOROV, V. I. BAKARIONOVA and V. N. MESHCHERJAKOV, "Failure modes in Composite IV," edited by J. A. Cornie and F. W. Crossman (Chicago, Illinois, 24–26 October 1977) pp. 285–96.
9. M. KH. SHORSHOROV, V. N. METCHERYAKOV, V. I. ZHAMNOVA, V. I. BAKARINOVA and I. A. POPOV, *Powder Met. Int.* 14 (1982) 41.
10. L. J. HOUSE, Thesis, May 1979, George Washington University, D.C.
11. A. G. METCALFE, Physical Chemical Aspects of the Interface, in "Metal Matrix Composites", edited by A. G. Metcalfe, Vol. 1, Chap. 3, pp. 65–121.
12. R. PAILLER, P. MARTINEAU, M. LAHAYE and R. NASLAIN, *Rev. Chim. Minéral.* 18 (1981) 520.
13. P. MARTINEAU, M. LAHAYE, R. PAILLER, R. NASLAIN, M. COUZI and F. CRUEGE, *J. Mater. Sci.* 19 (1984) 2731.
14. P. MARTINEAU, R. PAILLER and R. NASLAIN, *ibid.* 19 (1984).
15. H. E. DEBOLT, R. J. SUPLINSKA, J. A. CORNIE, T. W. HENZE and W. HAUZE, US Patent 4 340 636, 20 July (1982).
16. F. E. WAWNER, A. Y. TENG and S. R. NUTT, *SAMPE Quart.* 14(3) (1983) 39.

17. R. PAILLER, M. LAHAYE, J. THEBAULT and R. NASLAIN, in "Failure Modes in Composites-IV", edited by J. A. Cornie and F. W. Crossman (The Metallurgical Society of AIME, New York, 1979) pp. 265–84.
18. R. PAILLER, Thesis no. 616, University of Bordeaux I, France (1979).
19. C. E. BRUKL, in "Ternary Phase Equilibria in Transition Metal-Boron-Carbon-Silicon Systems", Part II, Vol. VII, Technical Report AFML-TR-65-2, US Department of Commerce, Nat. Tech. Inf. Serv., Springfield, Va.
20. W. JEITSCHKO and H. NOWOTNY, *Monat. Chem.* 98 (1967) 329.
21. J. SCHOENNAHL, B. WILLER and M. DAIRE, 4ème table ronde internationale sur le frittage, Dubrownik, Yougoslavie, 5–10 September (1977), pp. 338–45.
22. M. J. KLEIN, M. L. REID and A. G. METCALFE, Compatibility Studies for Viable Titanium Matrix Composites, Technical Report AFML-TR 69.242, US Department of Commerce, Nat. Tech. Inf. Serv. Springfield, Va.
23. J. THEBAULT, R. PAILLER, G. BONTEMPS-MOLEY, M. BOURDEAU and R. NASLAIN, *J. Less-Common Metal* 47 (1976) 221.
24. J. THEBAULT, Thesis no. 519, University of Bordeaux I, France (1977).

*Received 6 September*
*and accepted 22 September 1983*